Asian Journal of Chemistry; Vol. 38, No. 11 (2026), 2877-2882
ASIAN JOURNAL OF CHEMISTRY
https://doi.org/10.14233/ajchem.2026.35233

Characterization and Antimicrobial Activity of Silver Nanoparticles Obtained by Phytochemical Method Using *Anemone coronaria* Extract

KAINAT MUSLIM, BANU KESANLI and NUR PASAOGLULARI AYDINLIK*

Faculty of Arts and Sciences, Department of Basic Sciences and Humanities, Cyprus International University, Nicosia, North Cyprus, Mersin 10, Turkey

*Corresponding author: E-mail: nurp@ciu.edu.tr

Received: 11 November 2025 *Accepted*: 22 January 2026 *Published online*: 13 November 2026 AJC-22517

A safe, effective and environmentally-friendly technique for biosynthesis of Ag NPs in large quantities was achieved in this study. The ethanolic extract of *Anemone coronaria* was utilized for the first time to produce Ag NPs using a green method. The plant extract served as a stabilizing and reducing agent. The Ag NPs synthesized were extensively characterized using XRD analysis, SEM, zeta potential and UV-vis and FTIR spectroscopy. The initial appearance of UV-VIS absorbance peaks between 300 and 600 nm confirmed the formation of Ag NPs. Through XRD analysis, the synthesized Ag NPs' FCC geometry and crystalline shape were verified. The antimicrobial activities of the prepared nanoparticles against the bacteria *B. subtilis* and *E. coli* were assessed using the disk diffusion test. Compared to *B. subtilis*, Ag NPs seemed to have a stronger inhibitory effect on *E. coli*.

Keywords: Phytochemical, *Anemone coronaria* extract, Silver nanoparticles, Green chemistry, Reduction, Antimicrobial activity.

INTRODUCTION

The medicinal uses of silver have been documented in the literature going back to BC. At first, a large number of Greeks, Romans, Persians and Egyptians stored their food and water supplies in silver in one way or another as an antimicrobial substance. Silver was later used to treat wounds because of its effectiveness as an antimicrobial agent [1,2]. Silver nanoparticles (Ag NPs) have become increasingly useful in a variety of fields including electronics, medical devices, cosmetics, food technology, disinfectants, antimicrobial gels and paints, because of their advantageous physiochemical and antimicrobial activities [3-7]. Latest reports the use of Ag NPs as an anticancer agent as well [8]. Recently, as the commercial importance of Ag NPs has become apparent, green synthesis methods have been extensively explored. There are numerous ways to prepare Ag NPs, some of which are chemical reduction method, laser ablation method, synthesis using microorganisms and plant extracts [9]. Main disadvantage of the chemical and physical processes for producing Ag NPs is their high cost, usage of harmful compounds and potential biological and environmental risks [10].

The biological synthesis of Ag NPs using plant extracts has garnered attention due to its cost-effectiveness, accessibility, ease of use and environmental friendliness. One of the following could be used as a reducing agent to produce biologically synthesized nanoparticles *viz*. bacteria, fungi or plant/plant extract [11,12]. The plant's phytochemicals, which include catechins, tannins, polyphenols, isoflavones, flavonoids and flavones, function as reducing and stabilizing agents during the biosynthesis of Ag NPs. The best way to produce the required quality nanoparticles is to use common, easily accessible plants for the green synthesis of Ag NPs [13,14]. Thus, utilizing plant extracts for the production of Ag NPs is promising, since they are nontoxic and have a wide run of metabolites that can help reduce silver ions. The use of plant extracts as a reagent for nanoparticle synthesis has added benefit of being low-cost and efficient. There are many articles on synthesis of Ag NPs via phytochemical methods. Some examples include *aloe vera* [15], *nigella sativa* [16], ginkgo, magnolia and persimmon [17], *cannabis sativa* [18] and banana peel [19].

Due to their biocompatibility and regulated release of chemicals, green-synthesized nanoparticles have a wide range

This is an open access journal, and articles are distributed under the terms of the Attribution 4.0 International (CC BY 4.0) License. This license lets others distribute, remix, tweak, and build upon your work, even commercially, as long as they credit the author for the original creation. You must give appropriate credit, provide a link to the license, and indicate if changes were made.

of uses [20]. These nanoparticles have enormous potential for use in drug delivery systems [21], cancer therapy [22] and diagnostic imaging in the field of biomedicine. Nanoparticles are created *via* a variety of processes such as chemical, biological and physical ones. Plant extracts, organisms, enzymes, agricultural waste and synthesis facilitated by ultrasound and microwave technology are a few possible sources of green nanoparticles [23].

In this study, Ag NPs have been synthesized by using ethanolic extract of flowers of *Anemone coronaria via* phytochemical reduction method. *A. coronaria* is an herbaceous perennial plant, belonging to Ranunculaceae family, which is native to the Mediterranean region but could also be found in parts of North Africa and Near East [24]. Anemone species have been reported to have important biological activities including antimicrobial, anti-inflammatory, immunomodulatory and antioxidant activities as well as anticancer activities. The studies showed that saponins, flavonoids, steroids, lactones and triterpenoids are some of the phytochemicals present in *A. coronaria* [25]. This plant is widely abundant all over Cyprus from January till April month, which makes the plant readily available in bulk quantities and affordable for green chemistry studies. In addition, the phytochemicals present in *A. coronaria* such as flavonoids, triterpenoids and saponins are ideal reducing and capping agents in the biosynthesis of Ag NPs.

This research aims to contribute to systematic studies in exploring and utilizing accessible natural materials especially plants in the synthesis of nanoparticles. To our knowledge, this is the first report for green synthesis of Ag NPs by using ethanolic extract of *A. coronaria*, which serves as a novelty for this research. The complete characterization of the Ag NPs was achieved by employing ultraviolet visible spectroscopy (UV-Vis), scanning electron microscopy (SEM), Fourier transform infrared spectroscopy (FTIR) and X-ray diffraction (XRD) analysis. The antimicrobial activity of these Ag NPs was tested against *E. coli* (Gram-negative) and *B. subtilis* (Gram-positive) bacteria by using disk diffusion method.

EXPERIMENTAL

Plant extraction: *Anemone coronaria* fresh plants were collected from the Famagusta region (east coast of Cyprus) in March, 2022 (35.1384º N, 33.9592º E). The flower part of the plant was isolated, washed with distilled water, dried in air for 14 days and then ground to powder. The plant extract was obtained by dissolving 5 g of *A. coronaria* powder in 50 mL of ethanol in a conical flask. This was kept at room temperature for two days and then the green solution was filtered to obtain the ethanol extract.

Synthesis: A 1 mM silver nitrate ($AgNO_3$, Merck) solution was prepared by dissolving 0.017 g of $AgNO_3$ in 10 mL of distilled water, followed by dilution to a final volume of 100 mL in a volumetric flask. For nanoparticle synthesis, the 1 mM $AgNO_3$ solution and the ethanolic extract of *A. coronaria* were mixed in a 5:1 (v/v) ratio, wherein 50 mL of the $AgNO_3$ solution was combined with 10 mL of the plant extract under continuous stirring. Upon mixing, the reaction solution gradually changed to a pale yellow colour. Subsequent exposure to sunlight for 5 min intensified the colour to burgundy, indicating the reduction of Ag^+ ions to Ag^0 and the formation of silver nanoparticles, consistent with previously reported observations [26,27]. The resulting colloidal suspension was centrifuged at 4500 rpm for 20 min at 20 ºC to separate the nanoparticles. The collected precipitate was then dried in an oven at 45 ºC to obtain powdered Ag NPs for further characterization and analysis.

Characterization: UV-vis absorption analysis was done with Shimadzu UV-2450 instrument between 300 and 600 nm range. Fourier transform infrared spectrophotometer (FTIR) was done on a Shimadzu IR Prestige-21in the 4000-400 cm^{-1}. Joel JSM-6610LVinstrument was used for SEM analysis. Rigaku, Ultimate IV, powder X-ray diffractometer with 2θ range of 20-80º was used for XRD analysis. Zeta potential analysis was done by using Nano ZS (Malvern) instrument.

RESULTS AND DISCUSSION

UV-Vis spectroscopy: UV-visible spectroscopy was used to determine the maximum absorption of Ag NPs prepared from *A. coronaria* ethanol extract. The appearance of a peak at the wavelength of 385 nm and 495 nm with maximum absorbance confirms the formation of Ag NPs with smaller spherical Ag NPs primarily absorbs light while larger ones scatter more with peaks moving to longer wavelengths [11,28]. The peak around 495 nm exist as aggregates within a wire-like assembly, yet still connected to far larger clusters [23]. This aligns with its UV spectrum, as the broad shape indicates dispersion caused by aggregated assemblies with a low maximum absorption value as observed in Fig. 1.

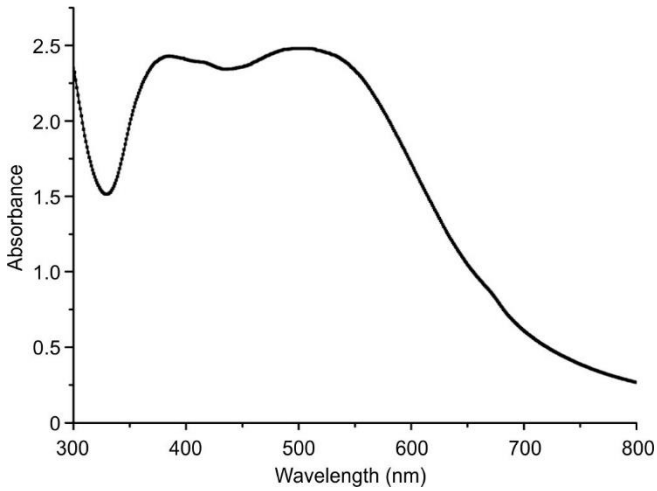


Fig. 1. UV-visible spectrum of Ag NPs synthesized with *A. coronaria* ethanol extract

FTIR spectrum: FT-IR spectroscopy was used in order to verify the formation of silver nanoparticles. FT-IR spectrum (Fig. 2) of Ag NPs synthesized and *A. coronaria* ethanol extract shows absorption bands at 3350 cm^{-1} and 3315 cm^{-1}, respectively representing-O-H and N-H stretching due to the presence of the surface water indicating presence of alcohols, phenols and amines [29]. The observed band around 1633 cm^{-1} corresponds to C=C stretching and N-H bending indicating presence of aromatic rings, alkenes and amides while FTIR

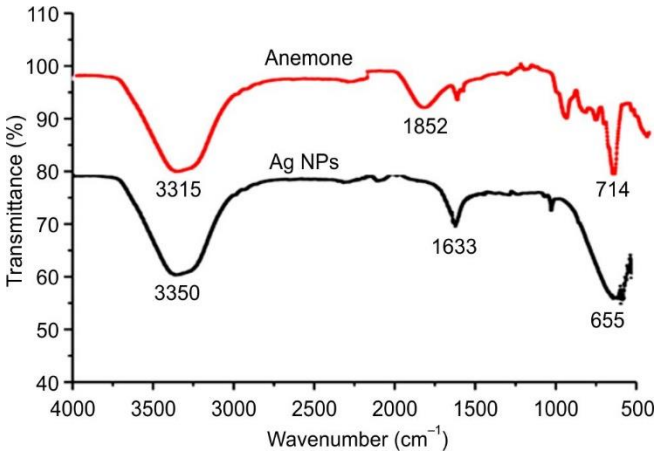


Fig. 2. FT-IR spectra of synthesized Ag NPs and *A. coronaria* extract

peaks of the extracts around 1852 cm^{-1} corresponds to C=O stretching of anhydride carbonyl. The stretching band at 655 cm^{-1} is most likely as a result of Ag-O bonds [30].

SEM morphology: In order to investigate the morphology of the Ag NPs synthesized *via* this phytochemical route, SEM technique was also used. The morphology of Ag NPs was studied using SEM sizing of 5 µm at resolution 5000X (Fig. 3). The powered form of Ag NPs under SEM appears spherical in shape although they seem to be in clusters of many crystallites due to agglomeration resulting in a larger particle size.

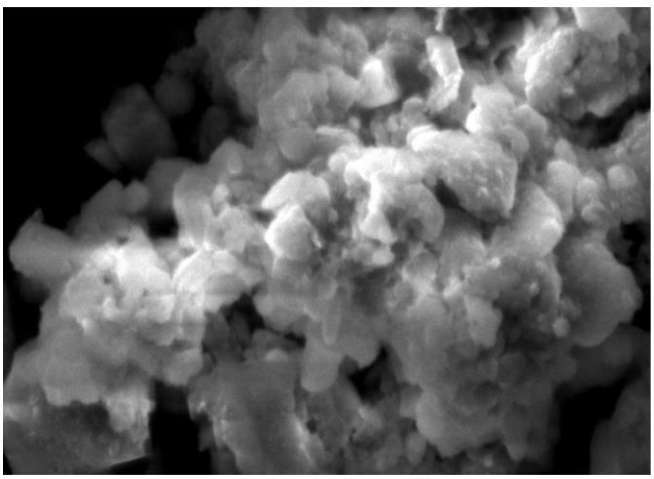


Fig. 3. SEM image of synthesized Ag NPs using *Anemone coronaria* extract

Zeta potential: Ag NPs prepared from *A. coronaria* ethanolic extract appears to have the average zeta potential distribution of 6.370 d·nm, zeta potential of -25.9 mV and polydispersity index (PDI) value of 0.505. PDI values higher than 0.4 indicate that the sample has a very broad particle size distribution and are polydisperse [31]. Thus, the nanoparticles for *A. coronaria* are polydisperse and zeta average shows that the Ag NPs are smaller in size. Zeta potential of nanoparticles with >+25 mV or <−25 mV usually shows high degree of stability. Fig. 4 shows *A. coronaria* zeta potential value is -25.9 mV and confirmed that the particles are highly stable [32].

Powder XRD analysis: Fig. 5 shows the XRD pattern of Ag NPs prepared from *A. coronaria* extract. Four different diffraction peaks can be seen at 2θ angle of 38.1º, 46.23º, 64.29º and 76.70º. These correspond to the (1 1 1), (2 0 0), (2 2 0) and (3 1 1) lattice planes, respectively, which are typical of face-centered cubic (fcc) structure of the nanoparticles (JCPDS No. 04-0873) [33]. Sharp peaks represent the crystalline shape of the Ag NPs. The lowest peak that is 76.70º near to 77º belongs to the plane (3 1 1) that confirms synthesis Ag NPs [34]. The crystallite size of the Ag NPs calculated based on Debye Scherrer's formula was found to be 35 nm [35].

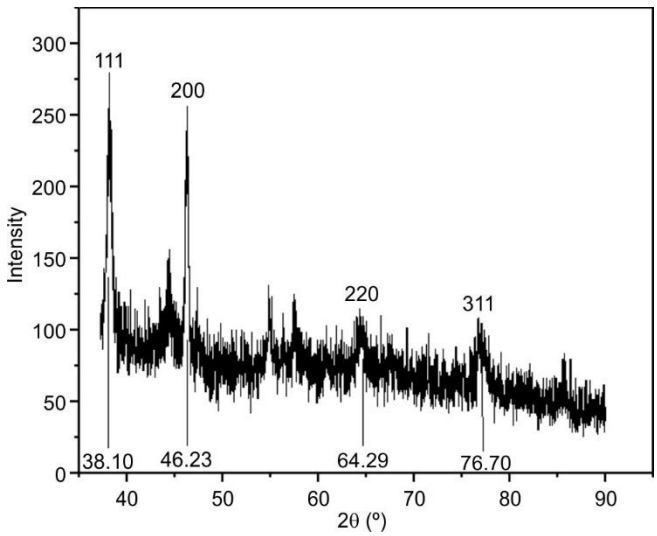


Fig. 5. XRD pattern of synthesized Ag NPs by *A. coronaria* extract

Antimicrobial activity: Antimicrobial applications of Ag NPs are currently being explored towards variety of treat-

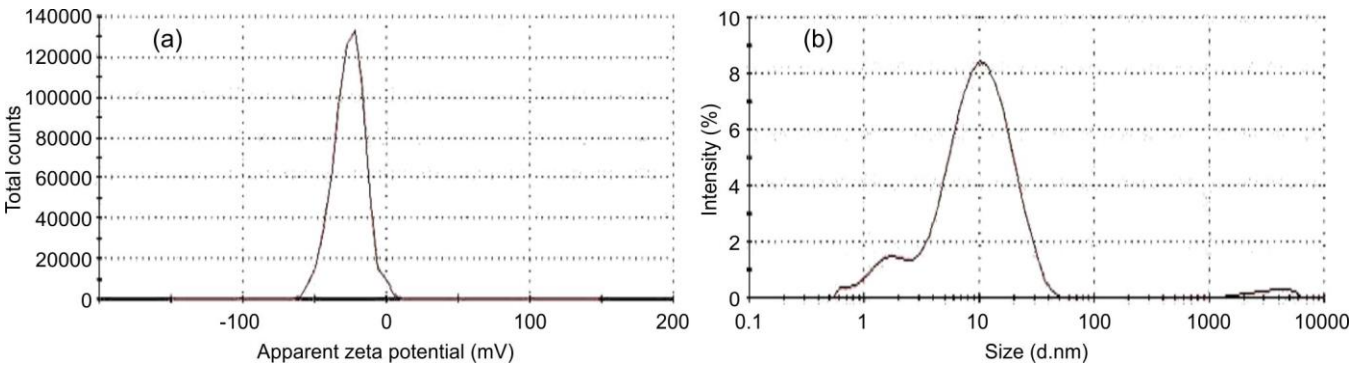


Fig. 4. (a) Zeta distribution potential and (b) zeta average and PDI value of the synthesized Ag NPs

ments. Ag NPs are reported to exhibit antibacterial activity towards both Gram-negative and Gram-positive bacteria [36-38]. The loaded antimicrobial discs contained 1 mM of the Ag NPs with *A. coronaria* extract, an indication for allowing higher Ag^+ ions release and interaction with bacterial membranes were carried out in duplicates. The antimicrobial activity of the Ag NPs prepared with *A. coronaria* ethanol extract has been tested in comparison to a standard antibiotic. The antibacterial activity results of Ag NPs, *A. coronaria* extract, $AgNO_3$ and gentamicin (standard antibiotic) against *B. subtilis* and *E. coli* are shown in Fig. 6. Ag NPs and $AgNO_3$ appeared to have a higher inhibitory effect on bacteria in contrast to the *A. coronaria* plant extract. The analyzed results also shows that there is a statistically significant difference between the results for *B. subtilis* ($p < 0.05$) and *E. coli* ($p < 0.05$). They all exhibit a higher antibacterial activity toward *E. coli* (Gram negative) as compared to the *B. subtilis* (Gram positive) bacteria as given in Fig. 6. Table-1 shows zone of inhibition by both microorganisms after 48 h.

Studies demonstrate that antibiotics exhibit enhanced antimicrobial effects when used in conjunction with Ag NPs [39]. This activity likely results from the enhanced ability of these antibiotics to penetrate cell walls when combined with nanoparticles. Antibiotic-nanoparticle combinations provide benefits that mitigate the adverse effects of broad-spectrum antibiotics. The benefits include increased local concentration of the antibiotic at the target site and enhanced binding to microorganisms [23]. Research shows that Ag NPs can disrupt cell membrane permeability, hinder respiration and increase free radical production; however, the exact mechanism of their antibacterial effect remains unclear. The antibacterial properties of Ag NPs result from the aforementioned factors [40]. The secondary metabolites in the ethanol extract of *A. coronaria* may facilitate cell membrane penetration. The mechanism of antimicrobial activity of biosynthesized Ag NPs is depicted in Fig. 7.

Comparison of *A. coronaria* mediated Ag NPs with other synthesized Ag NPs for antimicrobial activity: The antimicrobial activity of green synthesized Ag NPs from the ethanolic extract of *A. coronaria* compared to the previously synthesized Ag NPs as reported in literature is shown in Table-2.

Conclusion

Phytochemical reduction method by employing ethanolic extracts of *Anemone coronaria* was studied for a quick, affordable and more importantly, environmentally safe preparation of Ag NPs. The transformation of *A. coronaria* extract's colour into burgundy from light yellow, upon mixing with $AgNO_3$ under sunlight, was a clear indication of the formation of Ag NPs. The Ag NPs synthesized were furthermore characterized by UV-Vis, SEM, FT-IR, XRD and Zeta-potential. XRD analysis confirms the crystalline shapes of nanoparticles. Based on SEM result, the synthesized Ag NPs seem to have spherical shaped morphology. Ag NPs' preliminary bactericidal activity revealed their inhibitory action against both Gram-positive and Gram-negative bacteria. Growth of Gram-negative (*E. coli*) bacteria was, however, more severely restrained than the Gram- positive (*B. subtilis*) bacteria for plants extract and Ag NPs. Further investigation into the optimization of genetically modified microorganisms and a thorough toxicity assessment is necessary to fully realize the potential of green-synthesized nanoparticles.

CONFLICT OF INTEREST

The authors declare that there is no conflicts of interest regarding the publication of this article.

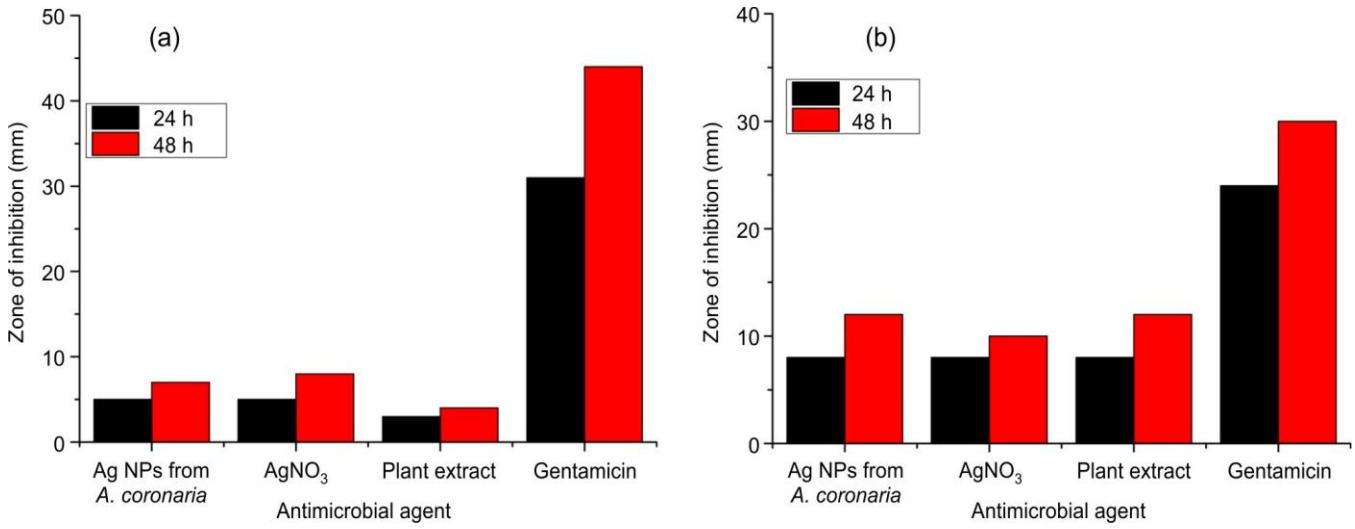


Fig. 6. Graphical illustration of the antimicrobial activity against (a) *B. subtilis* and (b) *E. coli* by *Anemone coronaria* extract and Ag NPs

TABLE-1
DISK DIFFUSION TEST RESULTS AFTER 48 h IN mm ARE GIVEN AND GENTAMICIN IS USED AS A REFERENCE ANTIBIOTIC

Microorganism	Ag NPs	$AgNO_3$	*Anemone coronaria* ethanolic extract	Gentamicin
B. subtilis (+)	7 (15.9%)	8 (18.2%)	4 (9.1%)	44 (100%)
E. coli (-)	12 (40%)	10 (33.3%)	12 (40%)	30 (100%)

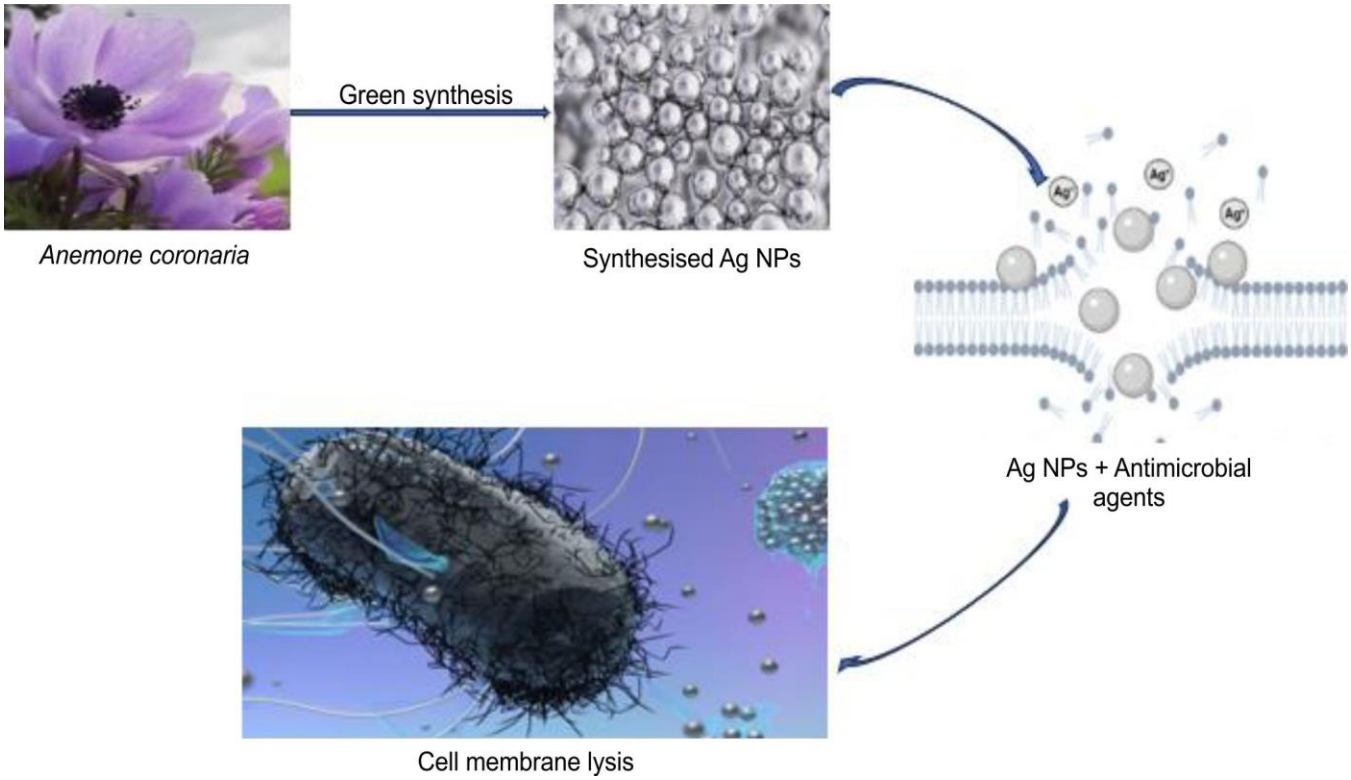


Fig. 7. Schematic illustration of the possible mechanism of the antimicrobial activity

TABLE-2
COMPARISON OF Ag NPs FROM *Anemone coronaria* WITH OTHER REPORTED SILVER NANOPARTICLES FOR ANTIMICROBIAL ACTIVITY

Ag NPs material	Method of synthesis	Microbial agents	Control antibiotic	Method of antimicrobial activity	Antimicrobial activity mechanism	Ref.
Bacillus amyloliquefaciens	One-step synthesis approach	*S. aureus*, *E. coli*, *P. aeruginosa*, *Salmonella*, *S. pyogenes* and *C. albicans*	Ciprofloxacin	Disk diffusion	Antimicrobial effect of biosynthesized silver nanoparticles was found to be size and shape dependent	[41]
Candida albicans	Biosynthesis	*S. aureus*, *E. coli*	Test compound	Disk diffusion	Association of silver with oxygen and its reaction with sulfhydryl groups on the cell wall to form R-S-S-R bonds	[42]
Aspergillus brasiliensis ATCC 16404	Mycosynthesis	*S. aureus*, *E. coli*	–	Disk diffusion	Mycosynthesized Ag NPs expressed good biocidal activity against different pathogenic micro-organisms	[43]
Brevibacterium frigoritolerans DC2	Biosynthesis	V. *parahaemolyticus*, *B. anthracis*, *S. enterica*	Vancomycin, penicillin	Well diffusion	Ag NPs have ability to damage the cell membrane permeability, damage the respiration functions of the cell and encourage the formation of free radicals.	[44]
Aspergillus niger	Fungal assisted biosynthesis	*Staphylococcus* sp., *Bacillus* sp. and *E. coli*	–	Disk diffusion	Ag NPs were preferentially bound and localized on the membrane of *E. coli* cells.	[45]
Streptomyces sp. SS2	Biosynthesis	*S. epidermis*, *B. subtilis*, *E. coli*	–	Disk diffusion	The antibacterial effect of Ag NPs is attributed to its small size and high surface to volume ratio	[46]
Dextran T40	Chemical reduction	*Pseudomonas aeruginosa*, *Bacillus cereus*, *Bacillus subtilis*, *E. coli*	–	Agar diffusion	The results confirmed that the treated *E. coli* cells are damaged, showing pit formation on bacterial cell walls.	[47]
Mango peel extract	Green synthesis	*S. aureus*, *E. coli*	–	Agar diffusion	The synthesized Ag NPs were all smaller than 150 nm, allowing easy absorption on the surface of the bacterial cell wall to react with the -NH- and -COOH functional groups of the peptidoglycan, corroding the cell wall.	[48]
Banana peel extract	Green synthesis	*B. subtilis*, *S. aureus*	Levofloxacin	Agar well diffusion	The high bactericidal activity of silver nanoparticles is due to their extremely large surface area, which provides better contact with microorganisms.	[49]
Anemone coronaria	Phytochemical method	*E. coli* and *B. subtilis* bacteria	Gentamicin	Disk diffusion	Inhibitory action against both Gram-positive and Gram-negative bacteria.	This study

DECLARATION OF AI-ASSISTED TECHNOLOGIES

The authors declare that no AI tools were used in the preparation or writing of this research/review article.

REFERENCES

1. J.W. Alexander, *Surg. Infect.*, **10**, 289 (2009); https://doi.org/10.1089/sur.2008.9941

2. S.S. Block, Disinfection, Sterilization and Preservation, Lippincott Williams & Wilkins: Philadelphia, PA, USA, edn 5, pp. 375-398 (2001).
3. S. Kumar, P. Kumar and C.S. Pathak, Silver Micro-Nanoparticles: Properties, Synthesis, Characterization, and Applications, IntechOpen: London, U.K. (2021).
4. H.D. Beyene, A.A. Werkneh, H.K. Bezabh and T.G. Ambaye, *Sustain. Mater. Technol.*, **13**, 18 (2017); https://doi.org/10.1016/j.susmat.2017.08.001
5. L. Xu, Y.Y. Wang, J. Huang, C.Y. Chen, Z.X. Wang and H. Xie, *Theranostics*, **10**, 8996 (2020); https://doi.org/10.7150/thno.45413
6. A.P. Patil, K.H. Kapadnis and S. Elangovan, *Mater. Sci. Res. India*, **18**, 143 (2021); https://doi.org/10.13005/msri/180203
7. M. Saravanan, S.K. Barik, D. MubarakAli, P. Prakash and A. Pugazhendhi, *Microb. Pathog.*, **116**, 221 (2018); https://doi.org/10.1016/j.micpath.2018.01.038
8. J.L. Mejía-Méndez, E.R. López-Mena and E. Sánchez-Arreola, *Biomedicines*, **11**, 389 (2023); https://doi.org/10.3390/biomedicines11020389
9. P. Nie, Y. Zhao and H. Xu, *Ecotoxicol. Environ. Saf.*, **253**, 114636 (2023); https://doi.org/10.1016/j.ecoenv.2023.114636
10. X. Li, H. Xu, Z.S. Chen and G. Chen, *J. Nanomater.*, **2011**, 1 (2011); https://doi.org/10.1155/2011/270974
11. K.S. Siddiqi, A. Husen and R.A. Rao, *J. Nanobiotechnology*, **16**, 14 (2018); https://doi.org/10.1186/s12951-018-0334-5
12. W.A. Shaikh, S. Chakraborty, G. Owens and R.U. Islam, *Appl. Nanosci.*, **11**, 2625 (2021); https://doi.org/10.1007/s13204-021-02135-5
13. A. Zuhrotun, D.J. Oktaviani and A.N. Hasanah, *Molecules*, **28**, 3240 (2023); https://doi.org/10.3390/molecules28073240
14. S. Bawazeer, A. Rauf, S.U.A. Shah, A.M. Shawky, Y.S. Al-Awthan, O.S. Bahattab, G. Uddin, J. Sabir and M.A. El-Esawi, *Green Process. Synth.*, **10**, 85 (2021); https://doi.org/10.1515/gps-2021-0003
15. P. Tippayawat, N. Phromviyo, P. Boueroy and A. Chompoosor, *Peer J.*, **4**, 2589 (2016); https://doi.org/10.7717/peerj.2589
16. R. Amooaghaie, M.R. Saeri and M. Azizi, *Ecotoxicol. Environ. Saf.*, **120**, 400 (2015); https://doi.org/10.1016/j.ecoenv.2015.06.025
17. J.Y. Song and B.S. Kim, *Bioprocess Biosyst. Eng.*, **32**, 79 (2009); https://doi.org/10.1007/s00449-008-0224-6
18. S. Chouhan and S. Guleria, *Mater. Sci. Energy Technol.*, **3**, 536 (2020); https://doi.org/10.1016/j.mset.2020.05.004
19. A. Bankar, B. Joshi, A.R. Kumar and S. Zinjarde, *Colloids Surf. A Physicochem. Eng. Asp.*, **368**, 58 (2010); https://doi.org/10.1016/j.colsurfa.2010.07.024
20. S. Loganathan, K. Selvam, G. Padmavathi, M.S. Shivakumar, S. Senthil-Nathan, A.G. Sumathi, M.A. Ali and S.M. Almutairi, *J. King Saud Univ. Sci.*, **34**, 18 (2022); https://doi.org/10.1016/j.jksus.2022.101846
21. C. Fang, Z. Ma, L. Chen, H. Li, C. Jiang and W. Zhang, *J. Photochem. Photobiol. B*, **190**, 72 (2019); https://doi.org/10.1016/j.jphotobiol.2018.11.011
22. M. Yusefi, K. Shameli, O.S. Yee, S.Y. Teow, Z. Hedayatnasab, H. Jahangirian, T.J. Webster and K. Kuča, *Int. J. Nanomedicine*, **16**, 2515 (2021); https://doi.org/10.2147/IJN.S284134
23. D. Kirubakaran, K. Selvam, P. Prakash, P. Manimegalai, M.S. Shivakumar and S. SenthilNathan, *Biotechnol. Appl. Biochem.*, **70**, 870 (2023); https://doi.org/10.1002/bab.2406
24. Flora of Cyprus, *Anemone coronaria*-Cyprus, [Online]. Available: https://floraofcyprus.com/ranunculales/anemone-coronaria-cyprus/ . (Accessed: Jan. 13, 2026).
25. D.C. Hao, X. Gu and P. Xiao, *Acta Pharm. Sin. B*, **7**, 146 (2017); https://doi.org/10.1016/j.apsb.2016.12.001
26. F. Narchin, K. Larijani, A. Rustaiyan, S. Nejad Ebrahimi and F. Tafvizi, *Adv. Pharm. Bull.*, **8**, 235 (2018); https://doi.org/10.15171/apb.2018.028
27. A. Baranwal, K. Mahato, A. Srivastava, P.K. Maurya and P. Chandra, *RSC Adv.*, **6**, 105996 (2016); https://doi.org/10.1039/C6RA23411A
28. P. Banerjee and D. Nath, *Nanosci. Technol.*, **2**, 1 (2015).
29. G. Singhal, R. Bhavesh, K. Kasariya, A.R. Sharma and R.P. Singh, *J. Nanopart. Res.*, **13**, 2981 (2011); https://doi.org/10.1007/s11051-010-0193-y
30. J. Rodriguez, *Surf. Sci.*, **296**, 149 (1993); https://doi.org/10.1016/0039-6028(93)91143-D
31. S. Bhattacharjee, *J. Control. Release*, **235**, 337 (2016); https://doi.org/10.1016/j.jconrel.2016.06.017
32. M. Horie and K. Fujita, Toxicity of Metal Oxide Nanoparticles, In: Advances in Molecular Toxicology, Elsevier, vol. 5, Chap. 4, pp. 145-178 (2011).
33. K. Roy, C.K. Sarkar and C.K. Ghosh, *Dig. J. Nanomater. Biostruct.*, **9**, 1137 (2014).
34. J. Das, M.P. Das and P. Velusamy, *Spectrochim. Acta A Mol. Biomol. Spectrosc.*, **104**, 265 (2013); https://doi.org/10.1016/j.saa.2012.11.075
35. B.D. Cullity and S.R. Stock, Elements of X-Ray Diffraction, Prentice Hall, edn 3 (2001).
36. J.R. Koduru, S.K. Kailasa, J.R. Bhamore, K.H. Kim, T. Dutta and K. Vellingiri, *Adv. Colloid Interface Sci.*, **256**, 326 (2018); https://doi.org/10.1016/j.cis.2018.03.001
37. I.A. Wani, T. Ahmad and A. Khosla, *Nanotechnology*, **32**, 462001 (2021); https://doi.org/10.1088/1361-6528/ac19d5
38. T. Bruna, F. Maldonado-Bravo, P. Jara, and N. Caro, *Int. J. Mol. Sci.*, **22**, 7202 (2021); https://doi.org/10.3390/ijms22137202
39. K. Lavanya, D. Kalaimurugan, M.S. Shivakumar and S. Venkatesan, *J. Cluster Sci.*, **31**, 265 (2020); https://doi.org/10.1007/s10876-019-01644-2
40. O.G. Kebede, N.P. Aydinlik, O.A. Oba and E. Ertekin, *Anal. Lett.*, **57**, 2773 (2024); https://doi.org/10.1080/00032719.2024.2302074
41. I. Ghiuță, D. Cristea, C. Croitoru, J. Kost, R. Wenkert, I. Vyrides, A. Anayiotos and D. Munteanu, *Appl. Surf. Sci.*, **438**, 66 (2018); https://doi.org/10.1016/j.apsusc.2017.09.163
42. T. Ahmad, I.A. Wani, N. Manzoor, J. Ahmed and A.M. Asiri, *Colloids Surf. B Biointerfaces*, **107**, 227 (2013); https://doi.org/10.1016/j.colsurfb.2013.02.004
43. B.A. Omran, H.N. Nassar, N.A. Fatthallah, A. Hamdy, E.H. El-Shatoury and N.S. El-Gendy, *J. Appl. Microbiol.*, **125**, 370 (2018); https://doi.org/10.1111/jam.13776
44. P. Singh, Y.J. Kim, H. Singh, C. Wang, K.H. Hwang, M.E.A. Farh, and D.C. Yang, *Int. J. Nanomedicine*, **2015**, 2567 (2015); https://doi.org/10.2147/IJN.S72313
45. L.R. Jaidev and G. Narasimha, *Colloids Surf. B Biointerfaces*, **81**, 430 (2010); https://doi.org/10.1016/j.colsurfb.2010.07.033
46. Y.K. Mohanta and S.K. Behera, *Bioprocess Biosyst. Eng.*, **37**, 2263 (2014); https://doi.org/10.1007/s00449-014-1205-6
47. K.P. Bankura, D. Maity, M.M. Mollick, D. Mondal, B. Bhowmick, M.K. Bain, A. Chakraborty, J. Sarkar, K. Acharya and D. Chattopadhyay, *Carbohydr. Polym.*, **89**, 1159 (2012); https://doi.org/10.1016/j.carbpol.2012.03.089
48. Y. Xing, X. Liao, X. Liu, W. Li, R. Huang, J. Tang, Q. Xu, X. Li and J. Yu, *Materials*, **14**, 5878 (2021); https://doi.org/10.3390/ma14195878
49. H.M. Ibrahim, *J. Radiat. Res. Appl. Sci.*, **8**, 265 (2015); https://doi.org/10.1016/j.jrras.2015.01.007